Properties of complexes H2C(X)P:PXH2, for X = F, Cl, OH, CN, NC, CCH, H, CH3, and BH2: P···P pnicogen bonding at σ-holes and π-holes

ARTICLE *in* THE JOURNAL OF PHYSICAL CHEMISTRY A · NOVEMBER 2013

Impact Factor: 2.69 · DOI: 10.1021/jp409016q · Source: PubMed

3 AUTHORS, INCLUDING:

Ibon Alkorta
Spanish National Research Council
679 PUBLICATIONS **12,371** CITATIONS
SEE PROFILE

José Elguero
Spanish National Research Council
1,502 PUBLICATIONS **22,122** CITATIONS
SEE PROFILE

THE JOURNAL OF PHYSICAL CHEMISTRY A

Article

pubs.acs.org/JPCA

Properties of Complexes $H_2C{=}(X)P{:}PXH_2$, for X = F, Cl, OH, CN, NC, CCH, H, CH_3, and BH_2: P···P Pnicogen Bonding at σ-Holes and π-Holes

Janet E. Del Bene,*[,†] Ibon Alkorta,*[,‡] and José Elguero[‡]

[†]Department of Chemistry, Youngstown State University, Youngstown, Ohio 44555 United States

[‡]Instituto de Química Médica (IQM-CSIC), Juan de la Cierva, 3, E-28006 Madrid, Spain

Supporting Information

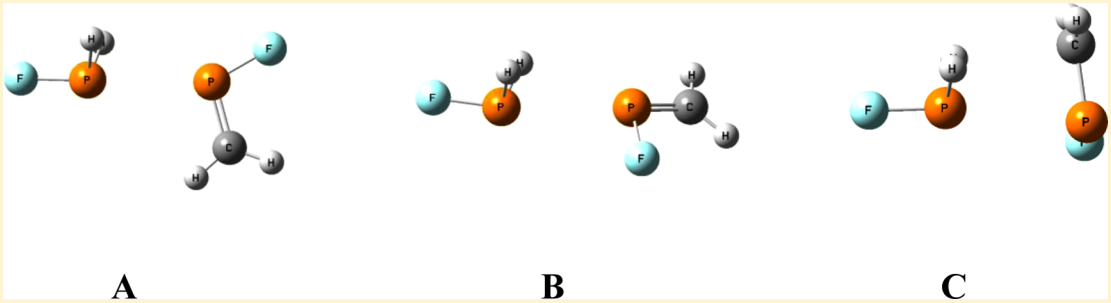

ABSTRACT: Ab initio MP2/aug′-cc-pVTZ calculations have been carried out on complexes $H_2C{=}(X)P{:}PXH_2$, for X = F, Cl, OH, CN, NC, CCH, H, CH_3, and BH_2. Three sets of complexes have been found on the potential surfaces. Conformation A complexes have A−P···P−A approaching linearity, with A the atom of X directly bonded to P. Conformation B complexes have A−P···P linear, but the P···P=C orientation of $H_2C{=}PX$ may differ significantly from linearity. Conformation C complexes are unique, since the pnicogen bond involves π-electron donation and acceptance by $H_2C{=}PX$. The order of binding energies of the three conformations of $H_2C{=}(X)P{:}PXH_2$ is C > A > B, with two exceptions. Although the binding energies of conformation C complexes tend to be greater than the corresponding conformation A complexes, intermolecular distances in conformation C tend to be longer than those in conformation A. Charge transfer stabilizes $H_2C{=}(X)P{:}PXH_2$ complexes. The preferred direction of charge transfer is from $H_2C{=}PX$ to PXH_2. In conformations A and B, charge transfer occurs from a P lone pair on one molecule to an antibonding σ^* orbital on the other. However, in conformation C, charge transfer occurs from the π orbital of $H_2C{=}PX$ to the σ^*P−A orbital of PXH_2, and from the lone pair on P of PXH_2 through the π-hole to the π^*P=C orbital of $H_2C{=}PX$. Changes in charges on P upon complexation do not correlate with changes in ^{31}P chemical shieldings. Computed EOM-CCSD spin−spin coupling constants correlate with P−P distances. At each distance, the ordering of ^{1p}J(P−P) is A > B > C. Binding energies and spin−spin coupling constants of conformation A complexes of $(PH_2X)_2$, $H_2C{=}(X)P{:}PXH_2$, and $(H_2C{=}PX)_2$ with A−P···P−A approaching linearity have been compared. For complexes with the more electronegative substituents, binding energies are ordered $(PH_2X)_2$ > $H_2C{=}(X)P{:}PXH_2$ > $(H_2C{=}PX)_2$, while the order is reversed for complexes formed from the more electropositive substituents. A plot of $\Delta E(PH_2X)_2/\Delta E(H_2C{=}PX)_2$ versus $\Delta E[H_2C{=}(X)P{:}PXH_2]/\Delta E(H_2C{=}PX)_2$ indicates that there is a systematic relationship among the stabilities of these complexes. Complexes $(PH_2X)_2$ tend to have larger spin−spin coupling constants and shorter P−P distances than $H_2C{=}(X)P{:}PXH_2$, which in turn have larger coupling constants and shorter P−P distances than $(H_2C{=}PX)_2$, although there is some overlap. Complexes having similar P−P distances have similar values of ^{1p}J(P−P).

INTRODUCTION

Subsequent to the landmark paper of Hey−Hawking et al.,[1] there has been a resurgence of interest in the pnicogen bond.[2−30] This bond arises when a pnicogen atom (N, P, As) acts as a Lewis acid by accepting a pair of electrons from a Lewis base. The great majority of studies thus far have used a phosphorus atom as the electron-pair acceptor. When two pnicogen atoms participate in forming a P···P or P···N bond, each pnicogen acts as both an electron-pair acceptor and an electron-pair donor. The great majority of studies of pnicogen bonds have involved the PH_3 molecule and its derivatives.

Although organophosphorus compounds with a double bond between carbon and phosphorus (R′R″C=PR) are not common, they are known, being first synthesized by Becker in 1976.[31] The geometries of the parent compound and some of its halogen derivatives have been described by Kroto and co-workers.[32−35] In a recent paper, we asked to what extent such a formally sp^2-hybridized P atom could participate in a P···P pnicogen bond in complexes $(H_2C{=}PX)_2$, for X = F, Cl, OH,

Received: September 9, 2013
Revised: October 13, 2013
Published: November 4, 2013

   dx.doi.org/10.1021/jp409016q | J. Phys. Chem. A 2013, 117, 11592−11604

CN, NC, CCH, H, CH_3, and BH_2.[30] This study yielded pnicogen bonded complexes with A−P···P−A or A−P···P=C approaching a linear arrangement, with A being the atom of X directly bonded to P, and C being the carbon of H_2C=PX. This study and our previous investigation of $(PH_2X)_2$ complexes led us undertake this investigation of the mixed binary complexes H_2C=(X)P:PXH_2. In this paper we report the structures, binding energies, bonding properties, and NMR properties of ^{31}P absolute chemical shieldings and ^{31}P−^{31}P spin−spin coupling constants for three different conformations of complexes H_2C=(X)P:PXH_2, for X = F, Cl, OH, CN, NC, CCH, H, CH_3, and BH_2. We also compare selected properties of H_2C=(X)P:PXH_2 complexes with linear A−P···P−A geometries to the corresponding complexes $(PH_2X)_2$ and $(H_2C$=$PX)_2$.

METHODS

The structures of the isolated monomers were optimized in previous studies at second-order Møller−Plesset perturbation theory (MP2)[36−39] with the aug′-cc-pVTZ basis set.[40] This basis set is derived from the Dunning aug-cc-pVTZ basis set[41,42] by the removal of diffuse functions from H atoms. The complexes H_2C=(X)P:PXH_2 were optimized at the same level of theory. Frequencies were computed to establish that the optimized structures correspond to equilibrium structures on their potential surfaces. Optimization and frequency calculations were performed using the Gaussian 09 program.[43]

The electron densities of the complexes have been analyzed using the Atoms in Molecules (AIM) methodology[44−47] and the Electron Localization Function (ELF),[48] employing the AIMAll[49] and Topmod[50] programs. The topological analysis of the electron density produces the molecular graph of each complex. This graph identifies the location of electron density features of interest, including the electron density (ρ) maxima associated with the various nuclei, saddle points which correspond to bond critical points (BCPs), and ring critical points which indicate a minimum electron density within a ring. The zero gradient line which connects a BCP with two nuclei is the bond path. The electron density at the BCP (ρ_{BCP}), the Laplacian of the electron density at the BCP ($\nabla^2\rho_{BCP}$), and the total energy density (H_{BCP}) are additional useful quantities which may be used to further characterize interactions.[51] The ELF function illustrates those regions of space at which the electron density is high. Using these measures, it is easy to identify bonds and lone pairs, and to characterize bond types.

The Natural Bond Orbital (NBO) method[52] has been used to obtain atomic charges and to analyze the stabilizing charge-transfer interactions in these binary complexes. The NBO-5 program[53] within the Gamess program[54] has been used for the NBO calculations.

Absolute chemical shieldings have been calculated for monomers and complexes at MP2/aug′-cc-pVTZ using the GIAO approximation.[55] Spin−spin coupling constants were evaluated using the equation-of-motion coupled cluster singles and doubles (EOM-CCSD) method in the CI (configuration interaction)-like approximation,[56,57] with all electrons correlated. For these calculations, the Ahlrichs[58] qzp basis set was placed on ^{13}C, ^{15}N, ^{17}O, and ^{19}F, the qz2p basis set was placed on ^{31}P and ^{35}Cl, and a previously developed hybrid basis set was placed on ^{11}B.[59] The Dunning cc-pVDZ basis set was placed on all H atoms except for a hydrogen-bonded H, in which case the qz2p basis set was used. Only ^1pJ(P−P) coupling constants are reported in this paper. The EOM-CCSD calculations were performed using ACES II[60] on the IBM Cluster 1350 (Glenn) at the Ohio Supercomputer Center.

RESULTS AND DISCUSSION

Although there are many minima on the H_2C=(X)P:PXH_2 surfaces, we have restricted our searches to regions that have structural characteristics associated previously with complexes stabilized by pnicogen bonds. We began by searching the region in which A−P···P−A approaches linearity, with A being the atom of X directly bonded to P. The resulting conformation A complexes are illustrated in Figure 1. We then investigated

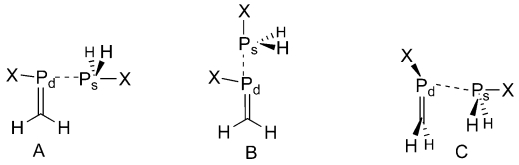

Figure 1. Conformations A, B, and C of H_2C=(X)P:PXH_2. P_d is the P atom which forms a double bond with the CH_2 group in H_2C=PX. P_s is the phosphorus which forms only single bonds in PH_2X.

the region in which A−P···P=C approaches linearity, with C being the carbon of H_2C=PX. These are labeled conformation B complexes. The results from this search led us to a third region, illustrated as conformation C in Figure 1. We did not search the regions in which one H of PH_2X assumes a linear arrangement, since $(PH_2X)_2$ complexes with linear H−P···P−H have significantly reduced binding energies relative to the same complexes with A−P···P−A linear.[18,23]

This section has been subdivided into four sections. The first section focuses on the properties of conformation A complexes. Complexes derived from conformation B are discussed in the second section, and conformation C complexes in the third. The final section presents a comparison of the binding energies and spin−spin coupling constants of conformation A complexes $(PH_2X)_2$, H_2C=(X)P:PXH_2, and $(H_2C$=$PX)_2$.

I. Conformation A Complexes. The structures, total energies, and molecular graphs of conformation A complexes with C_s symmetry are given in Table S1 of the Supporting Information. Intermolecular P−P and P_s−H_b distances, P···P−A and P···P=C angles, and binding energies are reported in Table 1, and a plot of ΔE versus the P−P distance is given in Figure 2. The relatively low correlation coefficient for the trendline is a result of the presence of a second interaction in some of these complexes in addition to the P···P pnicogen bond. This interaction involves the phosphorus of PH_2X (P_s) and the H atom of H_2C=PX which is closer to it (H_b). This interaction was observed previously in $(H_2C$=$PX)_2$ complexes, and was associated with those in which X is one of the less electronegative substituents. In complexes H_2C=(X)P:PXH_2, this interaction occurs in complexes with these same substituents, namely, CH_3, H, and BH_2. The molecular graphs of these complexes show the presence of this interaction as a bond path connecting P_s and H_b. Structurally, these three complexes are characterized by P_s−H_b distances of 3.260 Å or less, and P_s−P_d−C angles no greater than 86°. The structural differences between complexes with and without this interaction can be seen in Figure 3 by comparing H_2C=(F)-P:PFH_2 with H_2C=(BH_2)P:$P(BH_2)H_2$. Although the molecular graphs for complexes H_2C=(CCH)P:$P(CCH)H_2$ and H_2C=(CN)P:$P(CN)H_2$ do not have bond paths connecting P_s and H_b, their P_s−H_b distances and P_s−P_d=C angles suggest

dx.doi.org/10.1021/jp409016q | J. Phys. Chem. A 2013, 117, 11592−11604

Table 1. P−P and P_s−H_b Distances (R, Å), Binding Energies (ΔE, kJ/mol), and P_s−P_d=C, P_d−P_s−A, and P_s−P_d−A Angles (<, deg) of Conformation A Complexes H_2C=(X)P:PXH_2 with C_s Symmetry

X =	R(P−P)	ΔE	R(P_s−H_b)	<P_s−P_d=C	<P_d−P_s−A	<P_s−P_d−A
F	3.017	−17.11	3.548	106	180	149
Cl	3.099	−16.46	3.420	101	179	155
OH	3.204	−13.90	3.547	102	177	155
NC	3.228	−12.17	3.472	99	178	159
CCH	3.417	−13.39	3.306	91	180	168
CN	3.404	−10.22	3.358	92	176	168
CH_3	3.572	−10.22	3.260	86	175	171
H	3.600	−9.45	3.254	85	175	177
BH_2	3.736	−10.45	3.170	80	179	177

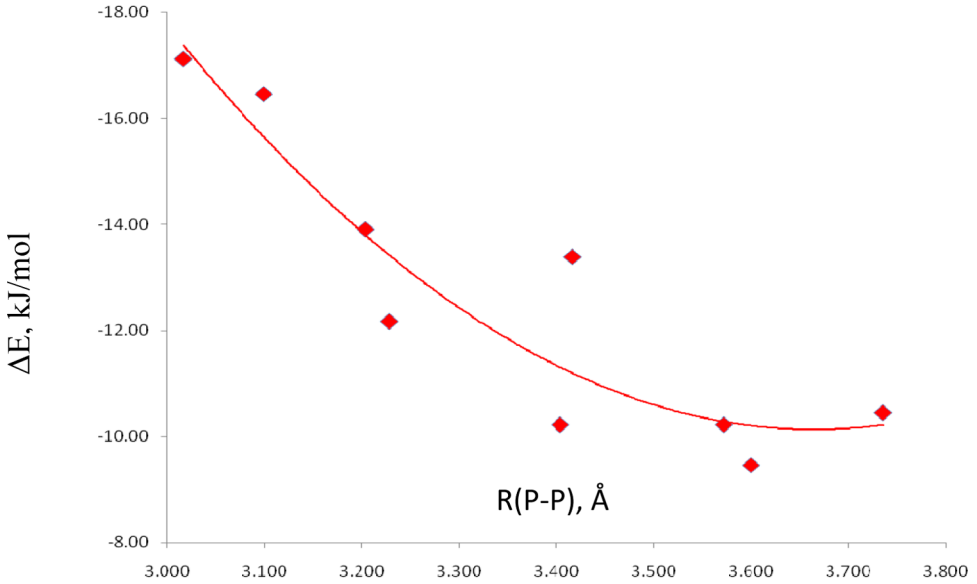

Figure 2. The binding energy (ΔE) versus the P−P distance. The second-order trendline has a correlation coefficient R^2 of 0.859.

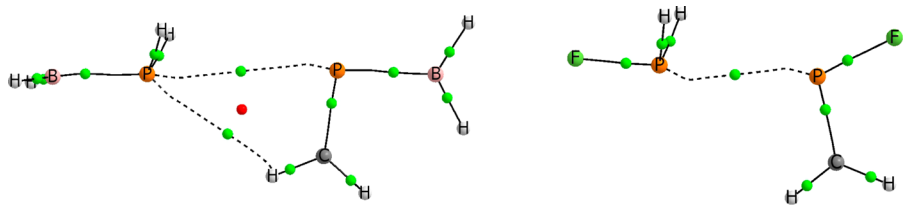

Figure 3. Structures and molecular graphs of conformation A complexes H_2C=(BH_2)P:$P(BH_2)H_2$ and H_2C=(F)P:PFH_2, indicating a P_s···H_b interaction in the former but not in the latter.

that a weak P_s···H_b interaction may still be present. There is a significant difference between the P_s−H_b distances and P_s−P_d=C angles in these complexes compared to those with F, Cl, OH, and NC as substituents. Thus, it is not surprising that there is not a good correlation between the P−P distances and the binding energies of conformation A complexes.

The charges on H_2C=PX and the stabilizing charge-transfer energies for complexes H_2C=(X)P:PXH_2 are reported in Table 2. In all complexes, charge transfer from the P_d lone pair to the σ^*P_s−A orbital is always more stabilizing than charge transfer from the lone pair of P_s to the σ^*P_d−A orbital. That is, charge transfer from H_2C=PX to PXH_2 is more favorable than the reverse process. This is consistent with the positive charge on H_2C=PX in these complexes, as indicated in Table 2. For complexes not having a strong P_s···H_b interaction, $P_d$lp→σ^*P_s−A charge-transfer energies range from 10.0 to 36.6 kJ/mol, while $P_s$lp→σ^*P_d−A charge-transfer energies range from 6.2 to 17.1 kJ/mol. For those complexes having this secondary interaction, the charge-transfer energies are much smaller and their range is reduced significantly, to 2.6 to 5.6 kJ/mol for $P_d$lp→σ^*P_s−A, and 0.2 to 3.4 kJ/mol for $P_s$lp→σ^*P_d−A.

The topological analysis of the electron densities of these complexes shows the presence of a bond critical point (BCP) and its associated P···P bond path in Table S1 of the Supporting Information. The values of the electron density at the BCP range between 0.006 and 0.022e. All complexes have positive values of the Laplacian at the BCP. However, the complexes with X = F, Cl, OH, and NC, which have the shortest P···P distances and the greatest binding energies, have negative total energy densities (H_{BCP}) at the BCPs. A negative value of H_{BCP} indicates that there is some degree of covalency in these interactions.

dx.doi.org/10.1021/jp409016q | J. Phys. Chem. A 2013, 117, 11592−11604

Table 2. NBO Charges (au) on $H_2C{=}PX$ and $P_d$lp→σ^*P_s–A and $P_s$lp→σ^*P_d–A Stabilizing Charge-Transfer Energies (kJ/mol) for Conformation A Complexes $H_2C{=}(X)P{:}PXH_2$[a]

$H_2C{=}(X)P{:}PXH_2$	charge on $H_2C{=}PX$	$P_d$lp→σ^*P_s–A	$P_s$lp→σ^*P_d–A
X = F	0.034	36.6	17.1
Cl	0.022	26.2	16.9
OH	0.019	21.7	9.8
NC	0.013	21.9	13.6
CCH	0.005	10.0	6.2
CN	0.005	10.8	7.6
CH_3	0.003	5.6	3.4
H	0.003	2.6	0.2
BH_2	0.002	2.6	0.9

[a] P_d refers to the phosphorus of $H_2C{=}PX$ and P_s to that of PH_2X (see Figure 1). A is the atom of X which is directly bonded to P.

The charges and absolute chemical shieldings of $^{31}P_d$ and $^{31}P_s$ are reported in Tables S2 and S3, respectively, of the Supporting Information. Table 3 presents the changes in these quantities upon formation of conformation A complexes. Although the positive charge on the $H_2C{=}P_dX$ molecule increases upon complexation, the positive charge on P_d decreases and the chemical shielding of P_d increases. A plot of the change in the absolute chemical shieldings versus the change in the charges on P_d has a second-order trendline with a correlation coefficient R^2 of only 0.736. While the plot indicates that the relatively small changes in the P_d chemical shieldings in $H_2C{=}(OH)P{:}P(OH)H_2$ and $H_2C{=}(F)P{:}PFH_2$ reflect the small changes in the positive charges on the P_d atoms, it also indicates that the change in the chemical shielding of P_d in $H_2C{=}(BH_2)P{:}P(BH_2)H_2$ is too small for a decrease of 0.020e in its positive charge. For the remaining six complexes, the increase in the chemical shieldings ranges from 45.2 to 49.1 ppm and is essentially independent of the decrease in the positive charge on P_d. Complexation also reduces the charge on P_s in PH_2X, and the P_s chemical shieldings increase, except for that of $H_2C{=}(OH)P{:}P(OH)H_2$ and $H_2C{=}(BH_2)P{:}P(BH_2)$-H_2. However, the best-fit second-order trendline has R^2 = 0.354, indicating that there is little correlation between these two variables for P_s in these complexes.

Table 3. Changes in Positive Charges (δe, au) and in Absolute Chemical Shieldings ($\delta\sigma$, ppm) of $^{31}P_d$ and $^{31}P_s$, and $^{31}P{-}^{31}P$ Spin–Spin Coupling Constants [^{1p}J(P–P), Hz] for Conformation A Complexes $H_2C{=}(X)P{:}PXH_2$

$H_2C{=}(X)P{:}PXH_2$	$\delta e(^{31}P_d)$	$\delta e(^{31}P_s)$	$\delta\sigma(^{31}P_d)$	$\delta\sigma(^{31}P_s)$	^{1p}J(P–P)
X = F	−0.004	−0.069	25.7	24.0	637.4
Cl	−0.023	−0.038	45.3	19.6	617.3
OH	−0.001	−0.026	5.1	−0.2	360.7
NC	−0.028	−0.038	49.1	15.8	427.8
CCH	−0.024	−0.023	47.8	9.4	210.4
CN	−0.032	−0.034	45.2	13.4	243.8
CH_3	−0.012	−0.010	45.7	10.0	105.9
H	−0.018	−0.013	48.6	19.5	100.7
BH_2	−0.020	−0.016	28.7	−8.4	47.1

$^{31}P{-}^{31}P$ spin–spin coupling constants across the pnicogen bond are also reported in Table 3. In previous papers, it has been demonstrated that the FC term is an excellent approximation to ^{1p}J(P–P). ^{1p}J(P–P) values and components have been computed for five of the complexes investigated in this study, and these are reported in Table S4 of the Supporting Information. These data indicate that the FC term approximates total J to about 1 Hz or less. Hence, it is the FC terms which will be used for comparison purposes.

Figure 4 provides a plot of ^{1p}J(P–P) versus the P–P distance. Although the binding energies of complexes $H_2C{=}(X)P{:}PXH_2$ do not correlate well with the intermolecular distances, it is evident from Figure 4 that ^{1p}J(P–P) does correlate with that distance. The trendline shown is a second-order polynomial with a correlation coefficient R^2 of 0.973. This good correlation suggests that experimental ^{1p}J(P–P) values could be used to estimate P–P distances. In our previous study of complexes $(H_2C{=}PX)_2$[30] it was also observed that binding energies do not correlate with intermolecular distances, but coupling constants across the pnicogen bonds do.

II. Conformation B Complexes. Table S1 of the Supporting Information reports the structures, total energies,

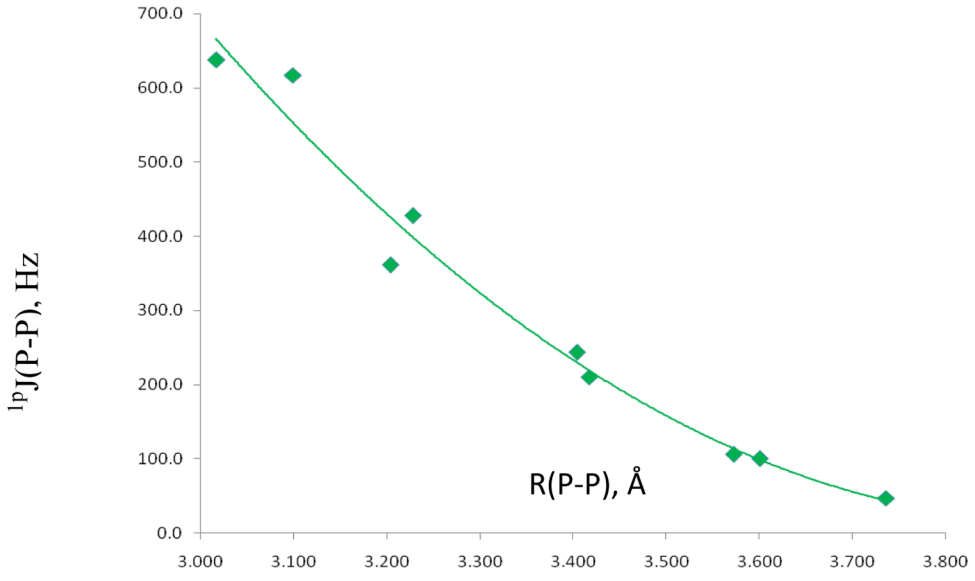

Figure 4. Coupling constants ^{1p}J(P–P) versus the P–P distance for conformation A complexes.

dx.doi.org/10.1021/jp409016q | J. Phys. Chem. A 2013, 117, 11592–11604

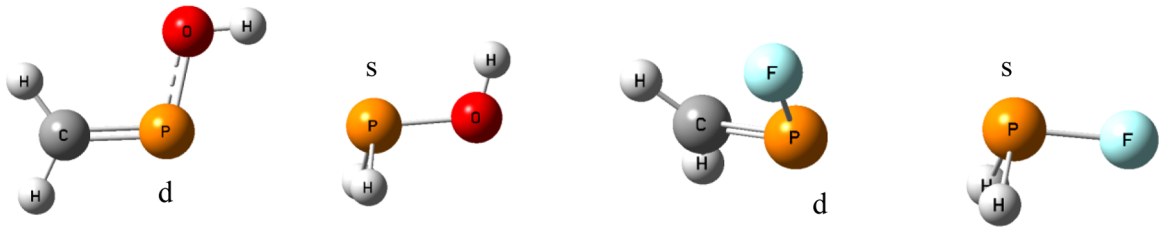

Figure 5. The structures of $H_2C{=}(OH)P{:}P(OH)H_2$ and $H_2C{=}(F)P{:}PFH_2$ in conformation B.

and molecular graphs of conformation B complexes. These complexes have C═P···P−A approaching linearity, with C being the carbon of $H_2C{=}PX$. However, only $H_2C{=}(OH)P{:}P(OH)H_2$ has an equilibrium planar structure stabilized by both a P···P pnicogen bond and an O−H···P_s hydrogen bond. The five remaining conformation B complexes have X = F, Cl, NC, CCH, and CN. Their equilibrium structures are nonplanar with C_1 symmetry, and are stabilized only by a pnicogen bond. Figure 5 illustrates the structures of $H_2C{=}(OH)P{:}P(OH)H_2$ and $H_2C{=}(F)P{:}PFH_2$. The three complexes missing from this set are $H_2C{=}(BH_2)P{:}P(BH_2)H_2$ which optimizes to a molecule with P−B bonds, $H_2C{=}(CH_3)P{:}P(CH_3)H_2$, and $H_2C{=}(H)P{:}PH_3$. The optimization of the latter two led to a different type of structure which will be discussed in section III.

The intermolecular P−P distances and binding energies of conformation B complexes are reported in Table 4. Not surprisingly, $H_2C{=}(OH)P{:}P(OH)H_2$ has the highest binding energy of −21.9 kJ/mol, significantly greater than any other conformation A or B complex. This complex is stabilized by an O−H···P_s hydrogen bond as well as a P···P pnicogen bond. Figure 6 presents a plot of the binding energies of conformation B complexes versus the intermolecular P−P distances. The red square represents $H_2C{=}(OH)P{:}P(OH)H_2$, and dramatically illustrates that its binding energy is much too high for its P−P distance, a result of the presence of the hydrogen bond. Excluding the point for $H_2C{=}(OH)P{:}P(OH)H_2$, the trendline is linear, but the correlation coefficient is only 0.67. Other types of curves have similar R^2 values between 0.64 and 0.67. A comparison of the binding energies in Tables 1 and 4 indicates that with the exception of $H_2C{=}(OH)P{:}P(OH)H_2$, conformation B complexes are less stable than the corresponding conformation A complexes.

The P_d−P_s−A, P_s−P_d−A, and P_s−P_d═C angles provide information about the geometry around the pnicogen bond in conformation A and B complexes. As noted in previous studies,[13,18] the P−P−A angles of $(PH_2X)_2$ and P−P−A or P−P−F angles of $(PHFX)_2$ tend to approach linearity, with A being the atom of X directly bonded to P. Supporting Information, Table S5 provides the values of these angles for complexes $(H_2C{=}PX)_2$ conformations A and B. In both conformations, the P_d−P_s−A angles which describe the geometry around the phosphorus which forms only single bonds tend toward linearity, varying from 175 to 180° in conformation A, and from 168 to 177° in conformation B. The value of this angle is closer to linearity in conformation A complexes compared to the corresponding conformation B, except for $H_2C{=}(OH)P{:}P(OH)H_2$, in which case the two conformations have the same value of 177°. However, the angles P_s−P_d−A and P_s−P_d═C which describe the geometry around the phosphorus which forms the C═P double bond show greater deviations from linearity, except for the conformation A complexes with the more electropositive substituents CH_3, H, and BH_2. Except for these, the P_s−P_d−A angles vary between 149 and 168°, while the P_s−P_d═C angles vary from 138 to 156°. The exception is the P_s−P_d═C angle in $H_2C{=}(OH)P{:}P(OH)H_2$ which is 179°, thereby facilitating the formation of the O−H···P_s hydrogen bond.

Table 4. Binding Energies (ΔE, kJ/mol), Intermolecular P−P Distances (R, Å), NBO Charges (au) on $H_2C{=}PX$, and $P_d$lp→σ^*P_s−A and $P_s$lp→σ^*P_d═C Stabilizing Charge-Transfer Energies (kJ/mol) of Conformation B Complexes $H_2C{=}(X)P{:}PXH_2$

X =	R	ΔE	$H_2C{=}PX$ charge	$P_d$lp→σ^*P_s−A	$P_s$lp→σ^*P_d═C
F	3.089	−13.84	0.036	31.7	8.9
Cl	3.172	−14.07	0.020	21.0	9.6
OH[a]	3.355	−21.86	−0.006	13.4	4.3[b]
NC	3.297	−10.75	0.011	17.2	5.8
CCH	3.423	−12.18	0.001	8.5	4.5
CN	3.463	−8.84	0.002	8.9	4.9

[a]Has C_s symmetry. All other complexes have C_1 symmetry. [b]Has an additional stabilizing P_s(lp) →σ^*O−H charge-transfer energy of 14.8 kJ/mol.

The NBO charges on $H_2C{=}PX$ and the stabilizing charge-transfer energies for conformation B complexes are reported in Table 4. As for the conformation A complexes, charge transfer from the P_d lone pair to the σ^*P_s−A orbital is always more stabilizing than charge transfer from the lone pair of P_s to the σ^*P_d═C orbital. This is consistent with the positive charges on $H_2C{=}PX$ in these complexes, except for $H_2C{=}(OH)P{:}P(OH)H_2$. In this complex, the dominant charge-transfer interaction is across the hydrogen bond, from P_s(lp)→σ^*O−H. This transition leads to a negative charge on $H_2C{=}POH$.

The P···P BCPs of conformation B complexes have smaller electron densities than those of the corresponding conformation A complexes. This is consistent with the longer P−P distances in conformation B, and with their smaller binding energies, except for $H_2C{=}(OH)P{:}P(OH)H_2$, which owes a significant part of its stability to the O−H···P_s hydrogen bond. Only the complexes with X = F and Cl have negative values of H_{BCP}, indicating that the P···P bonds in these two complexes have some degree of covalency. The degree of covalency is less in the conformation B complexes than in the corresponding A complexes.

Changes in the charges on the two P atoms and in their absolute chemical shieldings are reported in Table 5. Complex formation increases the chemical shieldings of P_d and P_s, and decreases the charge on these atoms except for P_d in $H_2C{=}(F)P{:}PFH_2$. For this complex the chemical shielding increases relative to the monomer, even though the positive charge also increases. A plot of the change in the chemical shielding versus the change in the positive charge shows a

dx.doi.org/10.1021/jp409016q | J. Phys. Chem. A 2013, 117, 11592−11604

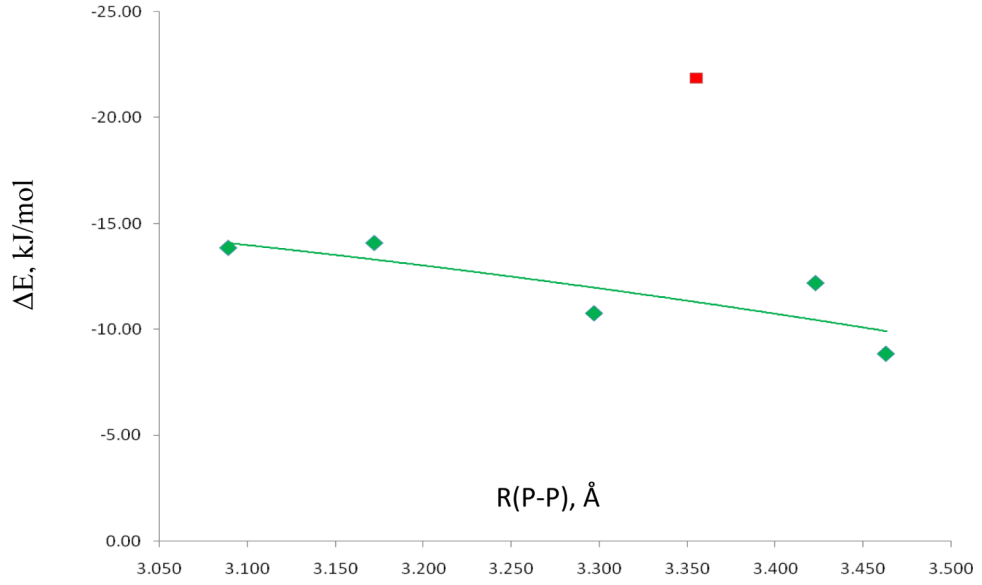

Figure 6. The binding energy (ΔE) versus the P−P distance for conformation B complexes. (red ■) $H_2C{=}(OH)P{:}P(OH)H_2$.

Table 5. Changes in Charges (e, au) and $^{31}P_d$ and $^{31}P_s$ Absolute Chemical Shieldings ($\delta\sigma$, ppm), and $^{31}P{-}^{31}P$ Spin−Spin Coupling Constants [^{1p}J(P−P), Hz] for Conformation B Complexes $H_2C{=}(X)P{:}PXH_2$

$H_2C{=}(X)P{:}PXH_2$	$\delta e(^{31}P_d)$	$\delta e(^{31}P_s)$	$\delta\sigma(^{31}P_d)$	$\delta\sigma(^{31}P_s)$	^{1p}J(P−P)
X = F	0.013	−0.057	25.4	25.5	364.8
Cl	−0.012	−0.022	42.3	16.4	319.5
OH	−0.004	−0.036	14.8	−8.9	174.6
NC	−0.017	−0.022	47.1	15.7	231.8
CCH	−0.011	−0.009	45.0	7.8	*a*
CN	−0.023	−0.014	43.1	14.6	181.0

[a]Value not available due to computational expense.

second-order trendline with a correlation coefficient of only 0.507. On this plot, it is evident that the point for $H_2C{=}(OH)P{:}P(OH)H_2$ is anomalous. Removing the point for this complex results in a second-order trendline with a correlation coefficient of 0.967. However, the curvature of this line is not realistic, since the curve reaches a maximum in the chemical shielding at approximately a −0.015e decrease in $\delta e(^{31}P_d)$. Increasing or decreasing the charge relative to this point leads to a decrease in $\delta\sigma(^{31}P_d)$. A similar situation occurs for $\delta\sigma(^{31}P_s)$ and $\delta e(^{31}P_s)$. Thus, there is no correlation between these two variables for either P atom.

Table 5 also reports the coupling constants ^{1p}J(P−P) and Figure 7 shows the expected correlation between ^{1p}J(P−P) and the P−P distance. It is interesting to note that although $H_2C{=}(OH)P{:}P(OH)H_2$ is structurally and energetically quite distinct from the remaining conformation B complexes, these differences do not influence the relationship between ^{1p}J(P−P) and the P−P distance. The second-order trendline shown in Figure 7 has a correlation coefficient R^2 of 0.961.

III. Conformation C Complexes. Table S1 of the Supporting Information reports the structures, total energies, and molecular graphs of conformation C complexes. Com-

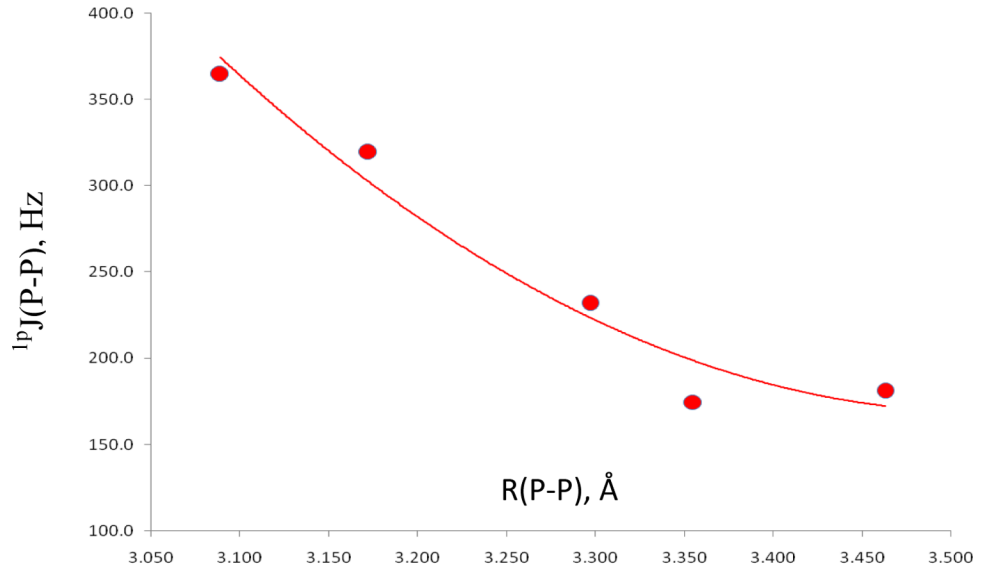

Figure 7. Coupling constants ^{1p}J(P−P) versus the P−P distance for conformation B complexes.

dx.doi.org/10.1021/jp409016q | J. Phys. Chem. A 2013, 117, 11592−11604

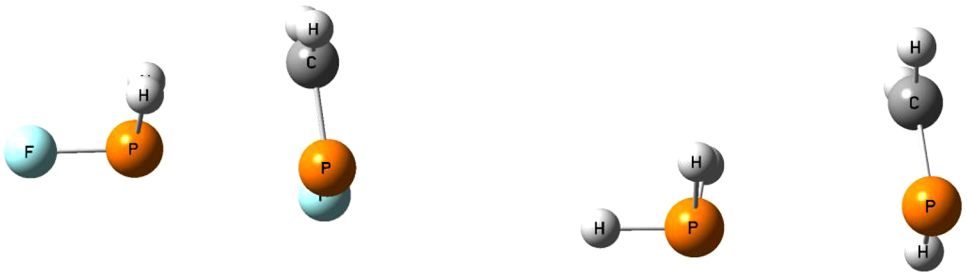

Figure 8. Structures of conformation C complexes $H_2C{=}(F)P{:}PFH_2$ and $H_2C{=}(H)P{:}PH_3$.

plexes of this type were first identified during the optimization of the conformation B complexes $H_2C{=}(CH_3)P{:}P(CH_3)H_2$ and $H_2C{=}(H)P{:}PH_3$. As noted above, the potential surfaces of these two binary complexes do not have equilibrium conformation B structures. Rather, the optimized structures have pnicogen bonds which involve π electron donation by $H_2C{=}PX$ to PH_2X through the σ-hole, and donation of the lone pair of PH_2X to $H_2C{=}PX$ through the π-hole. Optimization of the remaining complexes in this region of their potential surfaces yielded a set of conformation C complexes except for BH_2 as the substituent, in which case optimization led to a molecule with P−B bonds. To our knowledge, this is the first time that pnicogen bonded complexes with a π electron donor and π-hole acceptor involving the same π bond, have been reported. We will refer to this bond as a $\pi{-}\sigma$ pnicogen bond to indicate that it is the π system of one molecule and the σ system of the other that interact. It should be noted, however, that pnicogen bonds involving π electron donors and π-hole acceptors have been discussed in the literature, but the π donors and π-hole acceptors are not the same π bond.[7,21,29,61,62]

All conformation C complexes have $H_2C{=}PX$ nearly perpendicular to the plane defined by the P···P bond and the bisector of the $H{-}P_s{-}H$ angle. In addition, the values of the $P_s{-}P_d{=}C$ angles are between 76 and 85°, dramatically less than the values of these angles in conformation B complexes. These angular changes orient $H_2C{=}PX$ to interact through its π system with PH_2X. Since the C=P π bond is polarized toward C, $P_s{-}P_d{=}C$ angles less than 90° promote electron donation by $H_2C{=}PX$ through its π system at C, and lone-pair acceptance through the π-hole at P. The structures of conformation C complexes $H_2C{=}(F)P{:}PFH_2$ and $H_2C{=}(H)P{:}PH_3$ are illustrated in Figure 8.

The binding energies, intermolecular P−P distances, and $P_d{-}P_s{-}A$ and $P_s{-}P_d{=}C$ angles for conformation C complexes are reported in Table 6. These binding energies range from −8.2 for $H_2C{=}(H)P{:}PH_3$ to −20.0 kJ/mol for $H_2C{=}(F)P{:}PFH_2$. The order of binding energies of conformation C complexes is similar to that of conformation A complexes. However, $H_2C{=}(CCH)P{:}P(CCH)H_2$ is 1.2 kJ/mol more stable than $H_2C{=}(NC)P{:}P(NC)H_2$ in conformation A, but these two have essentially the same binding energies in conformation C. In addition, $H_2C{=}(CN)P{:}P(CN)H_2$ and $H_2C{=}(CH_3)P{:}P(CH_3)H_2$ have the same stabilities in conformation A, but $H_2C{=}(CH_3)P{:}P(CH_3)H_2$ is 0.8 kJ/mol more stable in conformation C. For the three conformations of complexes $H_2C{=}(X)P{:}PXH_2$, the order of binding energies is C > A > B with two exceptions. $H_2C{=}(OH)P{:}P(OH)H_2$ conformation B is the most stable complex in the entire set, but it is stabilized primarily by a strong O−H···P hydrogen bond and a pnicogen bond. $H_2C{=}(H)P{:}PH_3$ is 1.3 kJ/mol more stable in conformation A than in C. Although the binding energies of conformation C complexes tend to be greater than the corresponding conformation A complexes, intermolecular distances in conformation C are longer than those in conformation A, with two exceptions. The P−P distances in A and C conformations of $H_2C{=}(CH_3)P{:}P(CH_3)H_2$ are greater in A, while the P−P distances in conformations A and C of $H_2C{=}(H)P{:}PH_3$ are essentially the same. A plot of the binding energy versus the intermolecular distance for conformation C complexes is given in Figure 9. The second-order trendline has a correlation coefficient R^2 of 0.890.

Table 6. Binding Energies (ΔE, kJ/mol), Intermolecular P−P Distances (R, Å), and $P_d{-}P_s{-}A$ and $P_s{-}P_d{=}C$ angles (<, deg) for Conformation C Complexes $H_2C{=}(X)P{:}PXH_2$

X =	R	ΔE	$<P_d{-}P_s{-}A$	$<P_s{-}P_d{=}C$
F	3.029	−19.95	173	76
Cl	3.146	−19.63	174	77
OH	3.236	−17.57	175	77
NC	3.281	−15.19	174	77
CCH	3.456	−15.26	173	78
CN	3.528	−12.05	175	78
CH_3	3.484	−12.84	179	83
H	3.595	−8.18	175	85

Table 7 reports the NBO charges on $H_2C{=}PX$ and the stabilizing charge-transfer energies $\pi P_d{=}C{\rightarrow}\sigma^*P_s{-}A$ and $P_s$lp$\rightarrow\pi^*P_d{=}C$. As observed for both conformation A and conformation B complexes, charge transfer from $H_2C{=}PX$ to PH_2X is favored, although the nature of these transfers now involves π orbitals of $H_2C{=}PX$ in conformation C. Thus, the more stabilizing charge transfer occurs from the C=P π bond of $H_2C{=}PX$ to the σ^*P−A orbital of PH_2X, while charge transfer from the lone pair of PH_2X to the π^* orbital of $P_d{=}C$ is less stabilizing. This is consistent with the positive charges on $H_2C{=}PX$ in these complexes, except for $H_2C{=}(CCH)P{:}P(CCH)H_2$ and $H_2C{=}(CH_3)P{:}P(CH_3)H_2$ which have small negative charges on $H_2C{=}PX$. It is noteworthy that charge-transfer energies in a conformation C complex are greater than those in the corresponding conformation B. The single exception is found for charge transfer in $H_2C{=}(CN)P{:}P(CN)H_2$.

The electron density properties at the P···P BCPs have similar characteristics to those observed for conformation A and B complexes. The conformation C complexes with X = F, Cl, OH, and NC have negative values of H_{BCP}, indicating some covalency in the P···P bond. Moreover, there is an excellent correlation between the electron densities at P···P BCPs and the P−P distances in conformation A, B, and C complexes, in agreement with previous reports on pnicogen and other types

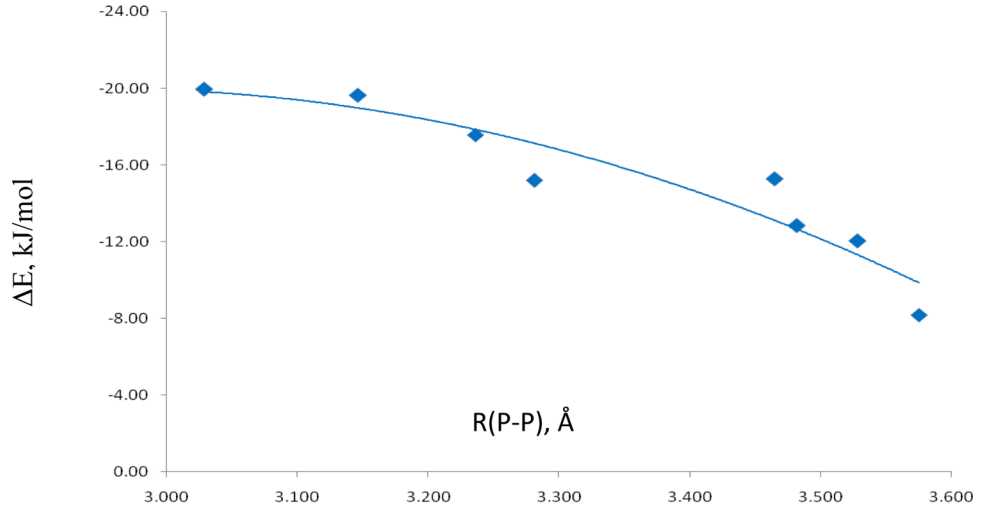

Figure 9. The binding energy (ΔE) versus the intermolecular P−P distance for conformation C complexes.

Table 7. NBO Charges (au) on $H_2C{=}PX$ and $\pi P_d{=}C{\rightarrow}\sigma^*P_s{-}A$ and $P_s lp{\rightarrow}\pi^*P_d{=}C$ Stabilizing Charge-Transfer Energies (kJ/mol) for Conformation C Complexes $H_2C{=}(X)P{:}PXH_2$

$H_2C{=}(X)P{:}PXH_2$	charge on $H_2C{=}PX$	$\pi P_d{=}C{\rightarrow}\sigma^*P_s{-}A$	$P_s lp{\rightarrow}\pi^*P_d{=}C$
X = F	0.010	34.9	16.7
Cl	0.016	29.3	11.6
OH	0.006	21.0	9.1
NC	0.007	18.9	7.8
CCH	−0.002	8.9	4.6
CN	0.002	8.0	3.3
CH_3	−0.003	7.9	5.1
H	0.001	6.8	4.4

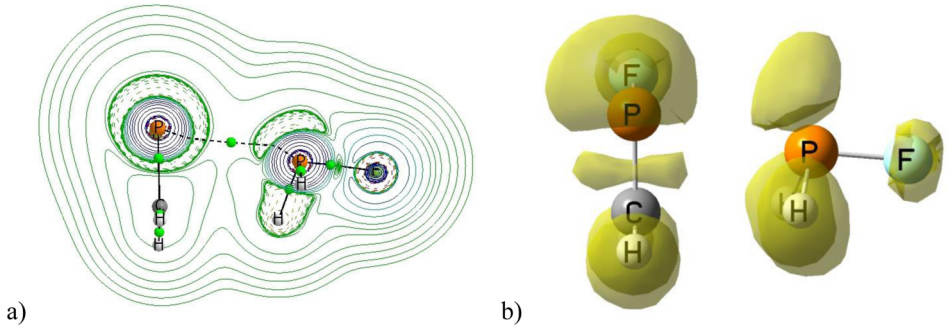

Figure 10. (a) The Laplacian contours and molecular graph of $H_2C{=}(F)P{:}PFH_2$. The contour plane is defined by the two P atoms and the BCP of the P···P bond. (b) The 0.8 au ELF isosurface of the $H_2C{=}(F)P{:}PFH_2$ conformation C complex.

of intermolecular interactions.[28,63−65] The Laplacian contours and molecular graph, and the ELF of $H_2C{=}(F)P{:}PFH_2$ are illustrated in Figure 10 panels a and b, respectively. They present a pictorial representation of the bond path and the disposition of the P_s lone pair and the π electrons which interact with the π- and σ-holes, respectively, consistent with the NBO description.

Changes in the charges on the two P atoms and in their absolute chemical shieldings are reported in Table 8. In contrast to conformation A and B complexes, the positive charge on P_d increases upon complex formation, while the charge on P_s decreases. However, the absolute chemical shieldings of both P_d and P_s increase upon complexation, except for the shieldings of P_s in $H_2C{=}(CH_3)P{:}P(CH_3)H_2$ and $H_2C{=}(CCH)P{:}P(CCH)H_2$. There is no correlation

Table 8. Changes in $^{31}P_d$ and $^{31}P_s$ Charges (δe, au) and Absolute Chemical Shieldings ($\delta\sigma$, ppm) and $^{31}P{-}^{31}P$ Spin−Spin Coupling Constants [$^{1p}J(P{-}P)$, Hz] for Conformation C Complexes $H_2C{=}(X)P{:}PXH_2$

$H_2C{=}(X)P{:}PXH_2$	$\delta e(P_d)$	$\delta e(P_s)$	$\delta\sigma(^{31}P_d)$	$\delta\sigma(^{31}P_s)$	$^{1p}J(P{-}P)$
X = F	+0.024	−0.041	49.4	59.5	105.1
Cl	+0.017	−0.015	50.5	30.8	125.7
OH	+0.020	−0.016	16.4	6.5	85.3
NC	+0.019	−0.021	49.9	24.0	79.2
CCH	+0.012	−0.009	44.3	0.0	*a*
CN	+0.014	−0.017	37.8	9.2	44.0
CH_3	+0.014	−0.006	40.6	−4.7	45.0
H	+0.009	−0.001	39.4	10.7	40.2

[a]Value not available because of computational expense.

dx.doi.org/10.1021/jp409016q | J. Phys. Chem. A 2013, 117, 11592−11604

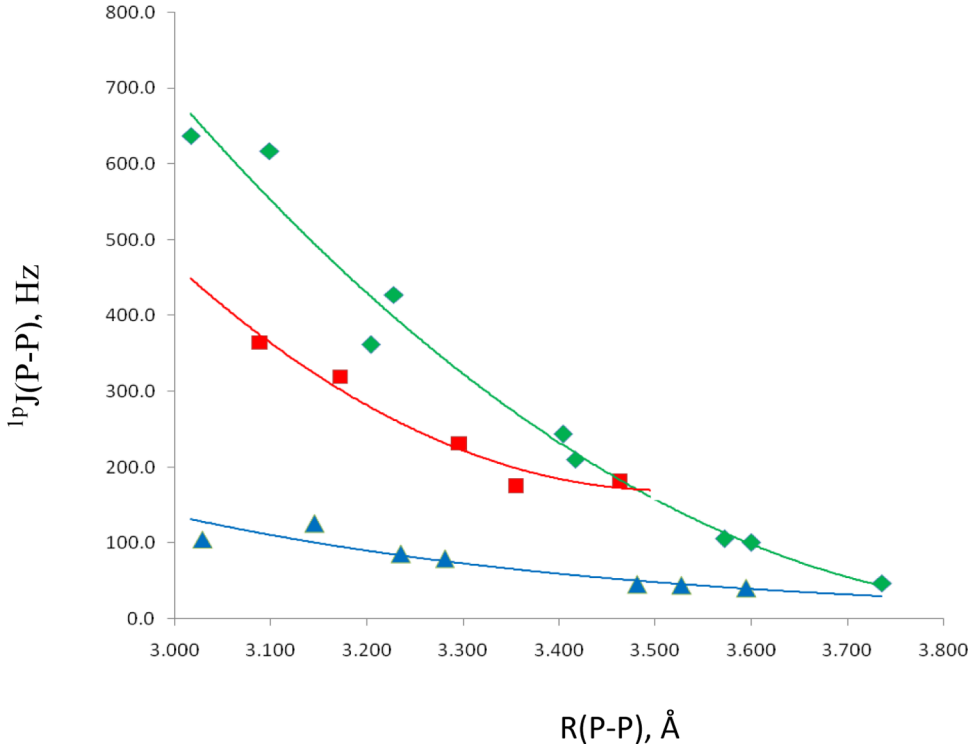

Figure 11. Coupling constants ^{1p}J(P−P) versus the P−P distance for conformation C (blue ▲) complexes. Coupling constants for conformation A (green ◆) and B (red ■) complexes are given for comparison.

Table 9. Binding Energies (Δ*E*, kJ/mol) of Complexes and the Ratios $\Delta E(PH_2X)_2/\Delta E(H_2C{=}PX)_2$ and $\Delta E[H_2C{=}(X)P{:}PXH_2]/\Delta E(H_2C{=}PX)_2$ for Complexes with A−P···P−A Approaching Linearity

X =	$(PH_2X)_2$[a]	$H_2C{=}(X)P{:}PXH_2$[b]	$(H_2C{=}PX)_2$[a]	$(PH_2X)_2/(H_2C{=}PX)_2$	$H_2C{=}(X)P{:}PXH_2/(H_2C{=}PX)_2$
F	−33.97	−17.11	−10.41	3.263	1.644
Cl	−22.09	−16.46	−13.33	1.657	1.235
OH	−20.55	−13.90	−9.45	2.175	1.471
NC	−13.76	−12.17	−11.06	1.244	1.100
CCH	−12.23	−13.39	−13.87	0.882	0.965
CH_3	−8.88	−10.22	−10.81	0.821	0.945
CN	−8.37	−10.22	−11.61	0.721	0.880
H	−7.08	−9.45	−11.16	0.634	0.847
BH_2	−7.04	−10.45	−13.52	0.521	0.773

[a] C_{2h} symmetry. [b] C_s symmetry.

between the change in the charge on P_d and the change in its chemical shielding upon complexation. The decrease in the positive charge and the increase in the chemical shielding of P_s are related by a second-order curve which has a correlation coefficient R^2 of only 0.791. Thus, it appears that at least in these pnicogen bonded complexes, the changes in the positive charge on the P atoms which form pnicogen bonds are not useful for predicting or understanding the changes in the chemical shieldings of these atoms.

Table 8 also reports the $^{31}P{-}^{31}P$ spin−spin coupling constants ^{1p}J(P−P) for conformation C complexes, and Figure 11 presents a plot of ^{1p}J(P−P) versus the intermolecular P−P distance for conformers A, B, and C. The usual second-order trendline has a correlation coefficient R^2 of 0.875 for conformation C. However, a decaying exponential, which has a correlation coefficient R^2 of 0.919, provides a better description of the relationship between ^{1p}J(P−P) and the P−P distance. The ordering of the trendlines for the three conformations is A > B > C. This ordering reflects the favorable A−P···P−A arrangement in A, followed by the A−P···P=C arrangement in B. Since the pnicogen bond is formed through the π system of $H_2C{=}PX$ in C and ^{1p}J(P−P) is essentially equal to the FC term which depends on s electron densities, conformation C complexes have the smallest values of ^{1p}J(P−P) at each P−P distance.

IV. Comparison of Binding Energies and Spin−Spin Coupling Constants of Complexes $(PH_2X)_2$, $H_2C{=}(X)P{:}PXH_2$, and $(H_2C{=}PX)_2$. To what extent are the properties of the mixed binary complexes $H_2C{=}(X)P{:}PXH_2$ related to those of the dimers $(PH_2X)_2$ and $(H_2C{=}PX)_2$? It is possible to make this comparison for all of the complexes of conformation A in which A−P···P−A approaches linearity, with A being the atom of X directly bonded to P. The binding energies of these complexes are reported in Table 9. These data indicate that for complexes in which X is one of the more electronegative substituents, the binding energies decrease from left to right, in going from $(PH_2X)_2$ to $H_2C{=}(X)P{:}PXH_2$ to $[H_2C{=}(X)P]_2$. For the more electropositive substituents, the binding energies

dx.doi.org/10.1021/jp409016q | J. Phys. Chem. A 2013, 117, 11592−11604

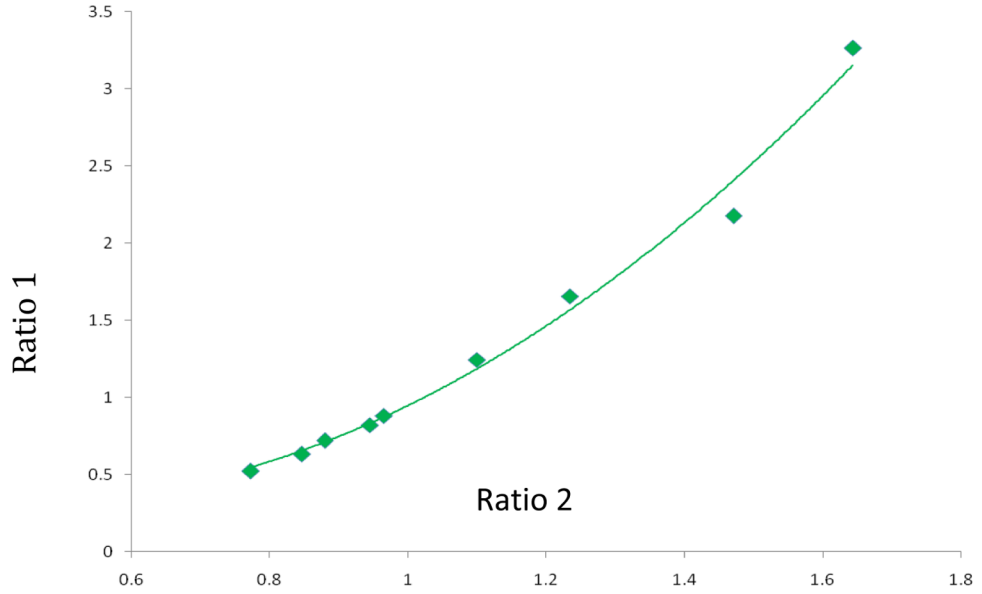

Figure 12. $\Delta E(PH_2X)_2/\Delta E(H_2C{=}PX)_2$ (Ratio 1) versus $\Delta E[H_2C{=}(X)P{:}PH_2X]/\Delta E(H_2C{=}PX)_2$ (Ratio 2) for corresponding complexes with A−P···P−A approaching linearity.

increase from left to right. Complexes $(H_2C{=}PX)_2$ with the substituents CCH, CH_3, H, and BH_2 have two P···H_b interactions in addition to the pnicogen bond which contribute to the total binding energy, and account for the different ordering of binding energies relative to $(PH_2X)_2$. What is quite interesting is the ratios of the binding energies $\Delta E(PH_2X)_2/\Delta E(H_2C{=}PX)_2$ and $\Delta E[H_2C{=}(X)P{:}PXH_2]/\Delta E(H_2C{=}PX)_2$, which are also reported in Table 9. In Figure 12, these ratios are plotted against each other. The trendline is a second-order polynomial with a correlation coefficient R^2 of 0.988. This plot indicates that there is a systematic relationship among the relative stabilities of the complexes $(PH_2X)_2$, $H_2C{=}(X)P{:}PXH_2$, and $(H_2C{=}PX)_2$ as a function of the substituent X, despite the fact that in some $H_2C{=}(X)P{:}PXH_2$ and $(H_2C{=}PX)_2$ complexes there are stabilizing interactions in addition to the P···P bond.

The second property of interest in conformation A complexes $(PH_2X)_2$, $H_2C{=}(X)P{:}PXH_2$, and $(H_2C{=}PX)_2$ with A−P···P−A approaching linearity is the one-bond spin−spin coupling constants $^{1p}J(P{-}P)$ as a function of the P−P distance. Table 10 reports the P−P distances for these complexes and $^{1p}J(P{-}P)$ values, and Figure 13 provides a plot of these variables. Although the shorter P−P distances are found in complexes $(PH_2X)_2$ and the longer distances in $(H_2C{=}PX)_2$, there is some overlap, as evident from Figure 13. The longest P−P distance in each series is found for the complex in which the substituent is BH_2. $^{1p}J(P{-}P)$ values vary from less than 50 Hz for $H_2C{=}(BH_2)P{:}P(BH_2)H_2$ and $(H_2C{=}PBH_2)_2$ to 1000 Hz for $(PH_2F)_2$ and 1100 Hz for $(PH_2Cl)_2$. It is these two points at the shortest distances and with the largest values of $^{1p}J(P{-}P)$ in Figure 13 which deviate most from the trendline. Nevertheless, complexes in these three series with similar P−P distances have similar values of $^{1p}J(P{-}P)$. That $^{1p}J(P{-}P)$ is a function of the P−P distance is evident from the trendline in Figure 13 which has a correlation coefficient R^2 of 0.929. Omitting $(PH_2Cl)_2$ leads to a correlation coefficient of 0.964; omitting $(PH_2F)_2$ leads to a correlation coefficient of 0.944.

Table 10. P−P Distances (R, Å) and $^{31}P{-}^{31}P$ Spin−Spin Coupling Constants [$^{1p}J(P{-}P)$, Hz] for $(PH_2X)_2$, $H_2C{=}(X)P{:}PXH_2$, and $(H_2C{=}PX)_2$ Conformation A Complexes with A−P···P−A Approaching Linearity

	$(PH_2X)_2$[a]		$H_2C{=}(X)P{:}PXH_2$[b]		$(H_2C{=}PX)_2$[a]	
X =	R	$^{1p}J(P{-}P)$	R	$^{1p}J(P{-}P)$	R	$^{1p}J(P{-}P)$
F	2.471	999	3.017	637	3.477	248
Cl	2.771	1120	3.099	617	3.373	330
OH	2.851	644	3.204	361	3.583	134
NC	3.040	640	3.228	428	3.422	264
CCH	3.353	282	3.417	210	3.510	140
CH_3	3.481	161	3.572	106	3.701	59
CN	3.375	300	3.404	244	3.456	187
H	3.589	131	3.600	101	3.618	75
BH_2	3.744	174	3.736	47	3.779	31

[a] C_{2h} symmetry. [b] C_s symmetry.

CONCLUSIONS

Ab initio MP2/aug′-cc-pVTZ calculations have been carried out on complexes $H_2C{=}(X)P_d{:}P_sXH_2$, with X = F, Cl, OH, CN, NC, CCH, H, CH_3, and BH_2. The results of these calculations support the following statements.

(1) Equilibrium conformation A complexes have $\sigma{-}\sigma$ pnicogen bonds and A−P···P−A approaching linearity, with A being the atom of X directly bonded to P. $\sigma{-}\sigma$ indicates that the σ systems of both atoms are involved in the pnicogen bond.

a. All conformation A complexes are stabilized by P···P pnicogen bonds, with binding energies varying between −10 and −17 kJ/mol. Complexes with the more electropositive substituents also have a stabilizing interaction between P_s of PXH_2 and H_b of $H_2C{=}PX$, with H_b being the H atom of the CH_2 group that is closer to P_s. As a result, binding energies and intermolecular P−P distances are not well correlated.

b. Charge transfer plays an important role in stabilizing these complexes. Charge transfer from the P_d lone pair of $H_2C{=}PX$ to the $\sigma^*P_s{-}A$ orbital of PXH_2 is more

dx.doi.org/10.1021/jp409016q | J. Phys. Chem. A 2013, 117, 11592−11604

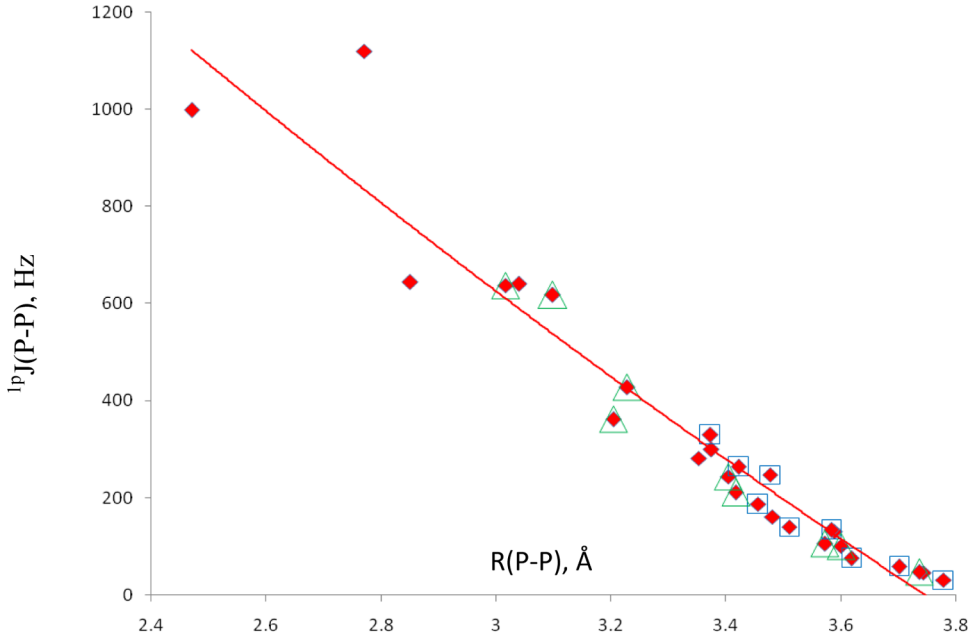

Figure 13. ^{1p}J(P−P) versus the P−P distance for conformation A (red ◆) complexes $(PH_2X)_2$, $H_2C{=}(X)P{:}PXH_2$, and $(H_2C{=}PX)_2$. (green △) $H_2C{=}(X)P{:}PXH_2$; (blue □) $(H_2C{=}PX)_2$.

stabilizing than charge transfer from the P_s lone pair to the σ^*P_d−A orbital.

c. There is no correlation between the changes in the charges on P upon complexation and the changes in the corresponding absolute chemical shieldings of ^{31}P. However, ^{1p}J(P−P) spin−spin coupling constants do correlate with the intermolecular P−P distance.

(2) Conformation B complexes have σ−σ pnicogen bonds in which A−P···P=C may approach linearity.

a. The most stable conformation B complex is $H_2C{=}(OH)P{:}P(OH)H_2$ which is stabilized by an O−H···P_s hydrogen bond and a P···P pnicogen bond. It has a planar C_s structure, and the largest binding energy among all $H_2C{=}(X)P{:}PXH_2$ complexes. The remaining equilibrium conformation B complexes have C_1 symmetry, and are formed only when X = F, Cl, NC, CCH, and CN. Except for $H_2C{=}(OH)P{:}P(OH)H_2$, conformation B complexes are less stable than corresponding A complexes. While the P_s−P_d−A angles in conformation A approach linearity, the P_d−P_s=C angles can deviate significantly from linearity.

b. Although changes in charges on P do not correlate with changes in chemical shieldings, ^{1p}J(P−P) coupling constants do correlate with P−P distances.

(3) Conformation C complexes have C_1 symmetry and are formed with all substituents except BH_2. The pnicogen bond in these complexes is unique, arising from π electron donation by $H_2C{=}PX$ through the σ-hole to the σ^*P_s−A orbital of PXH_2, and lone pair donation by P_s through the π-hole to the π^*P_d= C orbital of $H_2C{=}PX$. These are π−σ pnicogen bonds. π−σ indicates that the π system of one molecule interacts with the σ system of the other.

a. The binding energies of conformation C complexes are greater than the binding energies of the corresponding conformation A complexes, but the P−P distances in C are longer than the corresponding distances in A, with two exceptions.

b. For conformation C complexes, the stabilizing charge transfer energies $\pi P_d{=}C\rightarrow\sigma^*P$−A are greater than $P_s lp\rightarrow\pi^*P_d{=}C$.

c. As observed for conformations A and B, changes in charges on P do not correlate with changes in the ^{31}P chemical shieldings. However, ^{1p}J(P−P) does correlate with the P−P distance. On a plot of ^{1p}J(P−P) versus the P−P distance, the ordering of trendlines for the three conformations is A > B > C. At each distance, conformation C complexes have the smallest values of ^{1p}J(P−P). This may be attributed in part to the nature of the coupling constants which depend on s electron densities through the dominant Fermi-contact terms, and the nature of the interactions which involve the π electron systems of $H_2C{=}PX$.

(4) Binding energies and spin−spin coupling constants of complexes $(PH_2X)_2$, $H_2C{=}(X)P{:}PXH_2$, and $(H_2C{=}PX)_2$ may be compared for conformation A complexes with linear A−P··· P−A.

a. For complexes with the more electronegative substituents, binding energies are ordered $(PH_2X)_2$ > $H_2C{=}(X)P{:}PXH_2$ > $(H_2C{=}PX)_2$, while the order is reversed for complexes formed from the more electropositive substituents. This reversal may be attributed in part to the presence of P_s···H_b interactions in $H_2C{=}(X)$-$P{:}PXH_2$ and $(H_2C{=}PX)_2$. A plot of the ratios $\Delta E(PH_2X)_2/\Delta E(H_2C{=}PX)_2$ against $\Delta E[H_2C{=}(X)$-$P{:}PXH_2]/\Delta E(H_2C{=}PX)_2$ indicates that there is a systematic relationship among the relative stabilities of these complexes.

b. Complexes $(PH_2X)_2$ tend to have larger spin−spin coupling constants and shorter P−P distances than $H_2C{=}(X)P{:}PXH_2$, which in turn have larger coupling constants and shorter P−P distances than $(H_2C{=}PX)_2$, although there is some overlap. Nevertheless, complexes in these three series that have similar P−P distances have similar values of ^{1p}J(P−P).

dx.doi.org/10.1021/jp409016q | J. Phys. Chem. A 2013, 117, 11592−11604

■ ASSOCIATED CONTENT

Supporting Information

Molecular graphs, geometries, and energies of complexes $H_2C{=}(X)P{:}PXH_2$ conformations A, B, and C; NBO charges on P atoms in monomers and complexes; absolute chemical shieldings of ^{31}P in monomers and complexes; PSO, DSO, FC, and SD components of $^{1p}J(P-P)$; angles P_s-P_d-C and P_d-P_s-A in $(H_2C{=}PX)_2$ conformation A. This material is available free of charge via the Internet at http://pubs.acs.org.

■ AUTHOR INFORMATION

Corresponding Author

*E-mail: jedelbene@ysu.edu; ibon@iqm.csic.es.

Notes

The authors declare no competing financial interest.

■ ACKNOWLEDGMENTS

This work was carried out with financial support from the Ministerio de Economía y Competitividad (Project No. CTQ2012-35513-C02-02) and Comunidad Autónoma de Madrid (Project MADRISOLAR2, ref S2009/PPQ1533). Thanks are also given to the Ohio Supercomputer Center and CTI (CSIC) for their continued support.

■ REFERENCES

(1) Zahn, S.; Frank, R.; Hey−Hawkins, E.; Kirchner, B. Pnicogen Bonds: A New Molecular Linker? *Chem.—Eur. J.* **2011**, *17*, 6034−6038.

(2) Solimannejad, M.; Gharabaghi, M.; Scheiner, S. SH···N and SH···P Blue-Shifting H-Bonds and N···P Interactions in Complexes Pairing HSN with Amines and Phosphines. *J. Chem. Phys.* **2011**, *134* (024312), 1−6.

(3) Scheiner, S. A New Noncovalent Force: Comparison of P···N Interaction with Hydrogen and Halogen Bonds. *J. Chem. Phys.* **2011**, *134* (094315), 1−9.

(4) Scheiner, S. Effects of Substituents upon the P···N Noncovalent Interaction: The Limits of its Strength. *J. Phys. Chem. A* **2011**, *115*, 11202−11209.

(5) Adhikari, U.; Scheiner, S. Substituent Effects on Cl···N, S···N, and P···N Noncovalent Bonds. *J. Phys. Chem. A* **2012**, *116*, 3487−3497.

(6) Adhikari, U.; Scheiner, S. Sensitivity of Pnicogen, Chalcogen, Halogen and H-Bonds to Angular Distortions. *Chem. Phys. Lett.* **2012**, *532*, 31−35.

(7) Scheiner, S. Can Two Trivalent N Atoms Engage in a Direct N···N Noncovalent Interaction? *Chem. Phys. Lett.* **2011**, *514*, 32−35.

(8) Scheiner, S. Effects of Multiple Substitution upon The P···N Noncovalent Interaction. *Chem. Phys.* **2011**, *387*, 79−84.

(9) Scheiner, S. On the Properties of X···N Noncovalent Interactions for First-, Second-, and Third-Row X Atoms. *J. Chem. Phys.* **2011**, *134* (164313), 1−9.

(10) Adhikari, U.; Scheiner, S. Comparison of P···D (D = P, N) with other Noncovalent Bonds in Molecular Aggregates. *J. Chem. Phys.* **2011**, *135* (184306), 1−10.

(11) Scheiner, S.; Adhikari, U. Abilities of Different Electron Donors (D) to Engage in a P···D Noncovalent Interaction. *J. Phys. Chem. A* **2011**, *115*, 11101−11110.

(12) Scheiner, S. Weak H-Bonds. Comparisons of CHO to NHO in Proteins and PHN to Direct PN Interactions. *Phys. Chem. Chem. Phys.* **2011**, *13*, 13860−13872.

(13) Del Bene, J. E.; Alkorta, I.; Sánchez-Sanz, G.; Elguero, J. $^{31}P-^{31}P$ Spin−Spin Coupling Constants for Pnicogen Homodimers. *Chem. Phys. Lett.* **2011**, *512*, 184−187.

(14) Del Bene, J. E.; Alkorta, I.; Sánchez-Sanz, G.; Elguero, J. Structures, Energies, Bonding, and NMR Properties of Pnicogen Complexes $H_2XP{:}NXH_2$ (X = H, CH_3, NH_2, OH, F, Cl). *J. Phys. Chem. A* **2011**, *115*, 13724−13731.

(15) Adhikari, U.; Scheiner, S. Effects of Carbon Chain Substituents on the P···N Noncovalent Bond. *Chem. Phys. Lett.* **2012**, *536*, 30−33.

(16) Li, Q.-Z.; Li, R.; Liu, X.-F.; Li, W.-Z.; Cheng, J.-B. Pnicogen−Hydride Interaction between FH_2X (X = P and As) and HM (M = ZnH, BeH, MgH, Li, and Na). *J. Phys. Chem. A* **2012**, *116*, 2547−2553.

(17) Li, Q.-Z.; Li, R.; Liu, X.-F.; Li, W.-Z.; Cheng, J.-B. Concerted Interaction between Pnicogen and Halogen Bonds in $XCl{-}FH_2P{-}NH_3$ (X = F, OH, CN, NC, and FCC). *ChemPhysChem* **2012**, *13*, 1205−1212.

(18) Del Bene, J. E.; Alkorta, I.; Sánchez-Sanz, G.; Elguero, J. Structures, Binding Energies, and Spin−Spin Coupling Constants of Geometric Isomers of Pnicogen Homodimers $(PHFX)_2$, X = F, Cl, CN, CH_3, NC. *J. Phys. Chem. A* **2012**, *116*, 3056−3060.

(19) Del Bene, J. E.; Alkorta, I.; Sánchez-Sanz, G.; Elguero, J. Homo- and Heterochiral Dimers $(PHFX)_2$, X=Cl, CN, CH_3, NC: To What Extent Do They Differ? *Chem. Phys. Lett.* **2012**, *538*, 14−18.

(20) Alkorta, I.; Sánchez-Sanz, G.; Elguero, J.; Del Bene, J. E. Influence of Hydrogen Bonds on the P···P Pnicogen Bond. *J. Chem. Theor. Comp.* **2012**, *8*, 2320−2327.

(21) An, X.-L.; Li, R.; Li, Q.-Z.; Liu, X.-F.; Li, W.-Z.; Cheng, J.-B. Substitution, Cooperative, and Solvent Effects on π Pnicogen Bonds in the FH_2P and FH_2As Complexes. *J. Mol. Model.* **2012**, *18*, 4325−4332.

(22) Bauzá, A.; Quiñonero, D.; Deyà, P. M.; Frontera, A. Pnicogen-π Complexes: Theoretical Study and Biological Implications. *Phys. Chem. Chem. Phys.* **2012**, *14*, 14061−14066.

(23) Alkorta, I.; Sánchez−Sanz, G.; Elguero, J.; Del Bene, J. E. Exploring $(NH_2F)_2$, $H_2FP{:}NFH_2$, and $(PH_2F)_2$ Potential Surfaces: Hydrogen Bonds or Pnicogen Bonds? *J. Phys. Chem. A* **2013**, *117*, 183−191.

(24) Sánchez−Sanz, G.; Alkorta, I.; Elguero, J. Intramolecular Pnicogen Interactions in $PHF{-}(CH_2)n{-}PHF$ (*n* = 2−6) Systems. *ChemPhysChem.* **2013**, *14*, 1656−1665.

(25) Del Bene, J. E.; Alkorta, I.; Sánchez-Sanz, G.; Elguero, J. Phosphorus as a Simultaneous Electron−Pair Acceptor in Intermolecular P···N Pnicogen Bonds and Electron−Pair Donor to Lewis Acids. *J. Phys. Chem. A* **2013**, *117*, 3133−3141.

(26) Grabowski, S. J.; Alkorta, I.; Elguero, J. Complexes between Dihydrogen and Amine, Phosphine, and Arsine Derivatives. Hydrogen Bond versus Pnictogen Interaction. *J. Phys. Chem. A* **2013**, *117*, 3243−3251.

(27) Politzer, P.; Murray, J.; Clark, T. Halogen Bonding and Other σ-hole Interactions: A Perspective. *Phys. Chem. Chem. Phys.* **2013**, *15*, 11178−11189.

(28) Alkorta, I.; Elguero, J.; Del Bene, J. E. Pnicogen-Bonded Cyclic Trimers $(PH_2X)_3$ with X = F, Cl, OH, NC, CN, CH_3, H, and BH_2. *J. Phys. Chem. A* **2013**, *117*, 4981−4987.

(29) Sánchez-Sanz, G.; Trujillo, C.; Solimannejad, M.; Alkorta, I.; Elguero, J. Orthogonal Interactions between Nitryl Derivatives and Electron Donors: Pnictogen Bonds. *Phys. Chem. Chem. Phys.* **2013**, *15*, 14310−14318.

(30) Del Bene, J. E.; Alkorta, I.; Elguero, J. Characterizing Complexes with Pnicogen Bonds Involving sp^2 Hybridized Phosphorus Atoms: $(H_2C{=}PX)_2$ with X = F, Cl, OH, CN, NC, CCH, H, CH_3, and BH_2. *J. Phys. Chem. A* **2013**, *117*, 6893−6903.

(31) Becker, G. Bildung und Eigenschaften von Acylphosphinen. I. Monosubstitutionsreaktionen an substituierten Disilylphosphinen mit Pivaloylchlorid. *Z. Anorg. Allg. Chem.* **1976**, *423*, 242−254.

(32) Hopkinson, M. J.; Kroto, H. W.; Nixon, J. F.; Simmons, N. P. C. The Detection of Unstable Molecules by Microwave Spectroscopy: Phospha−Alkenes $CF_2{=}PH$, $CH_2{=}PCl$, and $CH_2{=}PH$. *Chem. Commun.* **1976**, 513−515.

(33) Kroto, H. W.; Nixon, J. F.; Ohno, K. The Microwave Spectrum of Phosphaethene, $CH_2{=}PH$. *J. Mol. Spectrosc.* **1981**, *90*, 367−373.

(34) Osman, O. I.; Whitaker, B. J.; Simmons, N. P. C.; Walton, D. R. M.; Nixon, J. F.; Kroto, H. W. The Microwave Spectrum 1-Chlorophosphaethene, $CH_2{=}PCl$. *J. Mol. Spectrosc.* **1984**, *103*, 113−124.

(35) Osman, O. I.; Whitaker, B. J.; Simmons, N. P. C.; Walton, D. R. M.; Nixon, J. F.; Kroto, H. W. The Microwave Spectrum of 1-

Fluorophosphaethene, CH_2=PF. *J. Mol. Spectrosc.* **1989**, *137*, 373−380.
(36) Pople, J. A.; Binkley, J. S.; Seeger, R. Theoretical Models Incorporating Electron Correlation. *Int. J. Quantum Chem., Quantum Chem. Symp.* **1976**, *10*, 1−19.
(37) Krishnan, R.; Pople, J. A. Approximate Fourth-Order Perturbation Theory of the Electron Correlation Energy. *Int. J. Quantum Chem.* **1978**, *14*, 91−100.
(38) Bartlett, R. J.; Silver, D. M. Many−Body Perturbation Theory Applied to Electron Pair Correlation Energies. I. Closed−Shell First−Row Diatomic Hydrides. *J. Chem. Phys.* **1975**, *62*, 3258−3268.
(39) Bartlett, R. J.; Purvis, G. D. Many−Body Perturbation Theory, Coupled−Pair Many-Electron Theory, and the Importance of Quadruple Excitations for the Correlation Problem. *Int. J. Quantum Chem.* **1978**, *14*, 561−581.
(40) Del Bene, J. E. Proton Affinities of Ammonia, Water, and Hydrogen Fluoride and their Anions: A Quest for the Basis-Set Limit Using the Dunning Augmented Correlation-Consistent Basis Sets. *J. Phys. Chem.* **1993**, *97*, 107−110.
(41) Dunning, T. H. Gaussian Basis Sets for Use in Correlated Molecular Calculations. I. The Atoms Boron through Neon and Hydrogen. *J. Chem. Phys.* **1989**, *90*, 1007−1023.
(42) Woon, D. E.; Dunning, T. H. Gaussian Basis Sets for use in Correlated Molecular Calculations. V. Core−Valence Basis Sets for Boron through Neon. *J. Chem. Phys.* **1995**, *103*, 4572−4585.
(43) Frisch, M. J.; Trucks, G. W.; Schlegel, H. B.; Scuseria, G. E.; Robb, M. A.; Cheeseman, J. R.; Scalmani, G.; Barone, V.; Mennucci, B.; Petersson, G. A.; Nakatsuji, H.; Caricato, M.; Li, X.; Hratchian, H. P.; Izmaylov, A. F.; Bloino, J.; Zheng, G.; Sonnenberg, J. L.; Hada, M.; Ehara, M.; Toyota, K.; Fukuda, R.; Hasegawa, J.; Ishida, M.; Nakajima, T.; Honda, Y.; Kitao, O.; Nakai, H.; Vreven, T.; Montgomery, J. A., Jr.; Peralta, J. E.; Ogliaro, F.; Bearpark, M.; Heyd, J. J.; Brothers, E.; Kudin, K. N.; Staroverov, V. N.; Kobayashi, R.; Normand, J.; Raghavachari, K.; Rendell, A.; Burant, J. C.; Iyengar, S. S.; Tomasi, J.; Cossi, M.; Rega, N.; Millam, J. M.; Klene, M.; Knox, J. E.; Cross, J. B.; Bakken, V.; Adamo, C.; Jaramillo, J.; Gomperts, R.; Stratmann, R. E.; Yazyev, O.; Austin, A. J.; Cammi, R.; Pomelli, C.; Ochterski, J. W.; Martin, R. L.; Morokuma, K.; Zakrzewski, V. G.; Voth, G. A.; Salvador, P.; Dannenberg, J. J.; Dapprich, S.; Daniels, A. D.; Farkas, O.; Foresman, J. B.; Ortiz, J. V.; Cioslowski, J.; Fox, D. J. *Gaussian−09*, Revision A.01; Gaussian, Inc.: Wallingford CT, 2009.
(44) Bader, R. F. W. A Quantum Theory of Molecular Structure and its Applications. *Chem. Rev.* **1991**, *91*, 893−928.
(45) Bader, R. F. W. *Atoms in Molecules, A Quantum Theory*; Oxford University Press: Oxford, UK, 1990.
(46) Popelier, P. L. A. *Atoms In Molecules. An Introduction*; Prentice Hall: Harlow, England, 2000.
(47) Matta, C. F.; Boyd, R. J. *The Quantum Theory of Atoms in Molecules: From Solid State to DNA and Drug Design*; Wiley-VCH: Weinheim, Germany, 2007.
(48) Silvi, B.; Savin, A. Classification of Chemical Bonds Based on Topological Analysis of Electron Localization Functions. *Nature* **1994**, *371*, 683.
(49) Keith, T. A., AIMAll (version 11.08.23), TK Gristmill Software, Overland Park KS, USA, 2011. http://aim.tkgristmill.com (accessed August 1, 2013).
(50) Noury, S.; Krokidis, X.; Fuster, F.; Silvi, B. TopMod Package, 1997.
(51) Rozas, I.; Alkorta, I.; Elguero, J. Behavior of Ylides Containing N, O, and C Atoms as Hydrogen Bond Acceptors. *J. Am. Chem. Soc.* **2000**, *122*, 11154−11161.
(52) Reed, A. E.; Curtiss, L. A.; Weinhold, F. Intermolecular Interactions from a Natural Bond Orbital, Donor−Acceptor Viewpoint. *Chem. Rev.* **1988**, *88*, 899−926.
(53) Glendening, E. D.; Badenhoop, J. K.; Reed, A. E.; Carpenter, J. E.; Bohmann, J. A.; Morales, C. M.; Weinhold, F. *NBO 5.G*; University of Wisconsin: Madison, WI, 2004.
(54) Schmidt, M. W.; Baldridge, K. K.; Boatz, J. A.; Elbert, S. T.; Gordon, M. S.; Jensen, J. H.; Koseki, S.; Matsunaga, N.; Nguyen, K. A.; Su, S. J.; Windus, T. L.; Dupuis, M.; Montgomery, J. A.*Gamess*, version 11; Iowa State University: Ames, IA, 2008.
(55) Ditchfield, R. Self-Consistent Perturbation Theory of Diamagnetism I. A Gauge-Invariant LCAO Method for NMR Chemical Shifts. *Mol. Phys.* **1974**, *27*, 789−807.
(56) Perera, S. A.; Nooijen, M.; Bartlett, R. J. Electron Correlation Effects on the Theoretical Calculation of Nuclear Magnetic Resonance Spin−Spin Coupling Constants. *J. Chem. Phys.* **1996**, *104*, 3290−3305.
(57) Perera, S. A.; Sekino, H.; Bartlett, R. J. Coupled−Cluster Calculations of Indirect Nuclear Coupling Constants: The Importance of Non−Fermi Contact Contributions. *J. Chem. Phys.* **1994**, *101*, 2186−2196.
(58) Schäfer, A.; Horn, H.; Ahlrichs, R. Fully Optimized Contracted Gaussian Basis Sets for Atoms Li to Kr. *J. Chem. Phys.* **1992**, *97*, 2571−2577.
(59) Del Bene, J. E.; Elguero, J.; Alkorta, I.; Yañez, M.; Mó, O. An ab Initio Study of ^{15}N-^{11}B Spin-Spin Coupling Constants for Borazine and Selected Derivatives. *J. Phys. Chem. A* **2006**, *110*, 9959−9966.
(60) Stanton, J. F.; Gauss, J.; Watts, J. D.; Nooijen, M.; Oliphant, N.; Perera, S. A.; Szalay, P. S.; Lauderdale, W. J.; Gwaltney, S. R.; Beck, S.; Balkova, A.; Bernholdt, D. E.; Baeck, K. K.; Tozyczko, P.; Sekino, H.; Huber, C.; Bartlett, R. J. *ACES II*, University of Florida: Gainesville, Fl.
(61) Solimannejad, M.; Nassirinia, N.; Amani, S. A Computational Study of 1:1 and 1:2 Complexes of Nitryl Halides (O_2NX) with HCN and HNC. *Struct. Chem.* **2013**, *24*, 651−659.
(62) Solimannejad, M.; Ramezani, V.; Trujillo, C.; Alkorta, I.; Sánchez-Sanz, G.; Elguero, J. Competition and Interplay between σ−Hole and π−Hole Interactions: A Computational Study of 1:1 and 1:2 Complexes of Nitryl Halides (O_2NX) with Ammonia. *J. Phys. Chem. A* **2012**, *116*, 5199−5206.
(63) Alkorta, I.; Elguero, J. Fluorine-Fluorine Interactions: A NMR and AIM Analysis. *Struct. Chem.* **2004**, *15*, 117−120.
(64) Tang, T. H.; Deretey, E.; Knak Jensen, S. J.; Csizmadia, I. G. Hydrogen Bonds: Relation Between Lengths and Electron Densities at Bond Critical Points. *Eur. Phys. J. D* **2006**, *37*, 217−222.
(65) Mata, I.; Alkorta, I.; Molins, E.; Espinosa, E. Universal Features of the Electron Density Distribution in Hydrogen-Bonding Regions: A Comprehensive Study Involving H···X (X = H, C, N, O, F, S, Cl, π) Interactions. *Chem.—Eur. J.* **2010**, *16*, 2442−2452.